II.3-SWB-NILE SIMPLE WATER BALANCE MODEL

This document is from 'A Simple Water Balance Model (SWB) for Estimating Runoff at Different Spatial and Temporal Scales' by J. C. Schaake, V. I. Koren, and Q. Y. Duan, Journal of Geophysical Research, Volume 101, March 20, 1996.

Introduction

The Simple Water Balance Model (SWB) is a parametric water balance model that was developed based on statistical averaging of the main hydrologic process.

The model has a 2 layer structure with both a physical and statistical basis for the model parameters. It was developed to fill a need for models with a small number of parameters and of intermediate complexity between a one parameter simple bucket and more complex hydrologically oriented models with many parameters such as the Sacramento Soil Moisture Accounting model. The focus was to improve the representation of runoff relative to the simple bucket without introducing the full complexity of the Sacramento model. The model was designed to operate over a range of time steps to facilitate coupling to an atmospheric model. The model can be used for catchment scale simulations in hydrological applications and for simple representation of runoff in coupled atmospheric/hydrological models.

An important role for the SWB model is to assist in understanding how much complexity in representing land surface processes is needed and can be supported with available data to estimate model parameters. The model was tested using rainfall, runoff and surface meteorological data for three catchments from different climate regimes. Model performance is compared to performance of a simple bucket model, the Sacramento model and the OSU land surface model. Finally a series of tests were conducted to evaluate the sensitivity of SWB performance when it is operated at time steps different from the time step for which it was calibrated.

Background

Complex hydrologic models such as the Sacramento Soil Moisture Accounting model were developed to represent spatially heterogeneous runoff processes for river basins at scales ranging from a few hundred to a few thousand KM2. They focus on the surface water budget and ignore aspects of the surface energy budget that are important for surface forcing in atmospheric models. These hydrologic models have parameters that must be calibrated with precipitation, discharge and surface meteorological data. To be useful in an atmospheric model these models must be coupled with a more complete treatment of the energy budget. Also a priori methods for parameter estimation must be developed for these models to apply to ungaged areas and to be used over the full domain of an atmospheric model.

Land surface parameterizations of existing atmospheric models focus on the surface energy budget and treat the surface water budget relatively simply (Carson, 1982; Lavel, 1988; Avissar and Verstraete, 1990). Some atmospheric model land surface parameterizations appear to be more physically based that most operational hydrologic models because they attempt to represent the water and energy processes in a vertical column of soil starting from the basic physical equations believed to govern those processes. Implicitly, it is assumed that there is an equivalent or effective vertical soil column that is representative of a large area. New land surface parameterizations such as BATS (Dickinson et al, 1993) and SiB (Sellers et al, 1986) are lumped models and represent vegetation as a 'big leaf'. Available land surface parameterizations do not account for important spatial heterogeneity in surface runoff processes and include parameters for which there is little supporting data (such as rooting depths and hydraulic properties of the soil).

In view of the limitations of existing hydrologic models and land surface parameterizations for atmospheric models a need existed for models with a small number of parameters and intermediate in complexity between a simple bucket, with only one parameter, and more complex hydrologically oriented models with many parameters such as the Sacramento model or some of the newer land surface models such as BATS and SiB with improved treatments of vegetation. By limiting the number of parameters, the potential to develop a priori parameter estimation techniques should be increased. A specific reason to develop the SWB model was to improve the representation of runoff relative to the simple bucket without introducing the full complexity of models such as the Sacramento model. Also the strategy was to keep the treatment of vegetation as simple as possible with the intention of adding features of more complex representations such as in BATS or SiB as seemed necessary based on tests with available data.

A goal is to use the SWB model together with other models to study the question of how much complexity is warranted in models of land surface processes. Recently, Jakeman and Hornberger (1993) studied this issue in the context of a simple rainfall-runoff model where the parameters of the model were identified (i.e. calibrated) using rainfall and runoff data. They conclude in reply to comments (Jakeman and Hornberger, 1994) that:

> '...conceptual and physically based models developed and used for describing rainfall-runoff processes tend to be over parameterized. They are no more useful for prediction than are simpler models whose parameters are identifiable from available data. If such overparameterized models are to be used to understand processes, then this must be achieved with remarkable care. On the other hand, the ability to produce identifiable models with about a half dozen parameters opens up opportunities to learn about how to generalize catchment response by studying a large number of catchments.'

Although SWB has only five parameters that can be identified by calibration from data readily available over parts of the United States, such data are available only for areas having stream gages

unaffected by upstream regulation and may apply only to the total area above these gages. Clearly, such data are not available for many potential (and ungaged) forecast points in the United States nor are they available globally.

SWB is being developed and tested as a contribution to the Global Water and Energy Cycle Experiment (GEWEX) Continental-scale International Project (GCIP) (WCRP,1992). GCIP has specific objectives to improve land surface models and to make better use of remotely sensed data. SWB has been coupled to the energy component of the OSU model and tested using data from the 1987 FIFE experiment (Mitchell et al, 1995, this issue). The coupled SWB-OSU model is being tested as part of the Project for Intercomparison of Land Surface Process Schemes (PILPS). SWB also is being applied in a stand-alone mode to estimate runoff from a number of river basins in the U.S. and in Africa (Koren, et al, 1995, this issue).

Model Development Strategy

New sources of hydrometeorological data such as radar, satellite and digital geographical information and a need to improve the land surface parameterization in atmospheric models has stimulated research into the spatial variability of hydrological processes (Russo and Bresler, 1981a,b; Vieira et al., 1981; Greminger et al., 1985; Thomas and Henderson-Sellers, 1987; Wood et al., 1988). This has led to the development of more general hydrological models with distributed model features (Entekhabi and Eagleson, 1989; Smith et al., 1992; Famiglietti and Wood, 1994; Chen et al., 1994).

The water and energy fluxes that must be represented in an atmospheric model may be divided into storm periods and inter-storm periods. During storm periods the water branch of the hydrologic cycle is dominant and the physics governing the partitioning of precipitation into interception, surface runoff and infiltration is highly non-linear. During inter-storm periods, the energy branch of the hydrologic cycle is dominant and the physics governing the partitioning of energy into sensible and latent heat fluxes into the atmosphere, while non-linear, is more nearly linear than water flux partitioning during storm periods. SWB must represent both storm and inter-storm periods, but the main focus on representing the effects of spatial heterogeneity in SWB is on processes during storm periods.

In some atmospheric models, basic equations of physics that might apply to a vertical column of soil are assumed to apply over large areas. Implicitly this assumes the relevant processes are nearly linear and parameters are spatially almost constant. Because the processes governing the split of water between infiltration and runoff are highly non-linear, such assumptions usually do not hold at large scales.

Ideally it might seem desirable to construct an improved land surface process model beginning with the basic computational element of a distributed model to represent basic physical processes at a point or for a hillslope or for a small representative elementary area. Parameters of equations used at this scale would appear to have clear

physical meaning and may be observable (at least locally) in field experiments. The aggregate behavior of the land surface processes at the scale of an atmospheric model could be obtained from the aggregate behavior of the distributed model.

However this strategy produces major problems. First the basic physics apply only at a point. There is no agreement in the scientific community on the aggregate equations governing processes for hillslopes or small elementary areas. Second integration of the fundamental equations of physics starting from point processes, explicitly in space and time, requires more information about the 3-dimensional heterogeneity of surface characteristics and 2-dimensional characteristics of surface forcing than is possible to measure. In principle such measurements would be unique to each catchment and each hydrologic event. Until a general theory to account for the uncertainty and heterogeneity in surface characteristics and processes is developed, simple approaches such as used to develop the SWB are needed.

Derived Probability Distributions of Land Surface Processes

The SWB is based on relationships between spatially averaged fluxes and state variables assuming that surface processes locally behave according to 'physically based‹ rules. This approach considers the frequency of occurrence of variables of certain ranges over an area without regard to the location of a particular occurrence within the area. Areal variables can be calculated as the statistical expectation of point values in this case. The 'physically based‹ rules used to develop SWB consider the basic physical processes but not at the level of systematic derivation from first principles.

The probability-distributed principle in hydrology was first used in modeling of the snowmelt processes. Komarov (1959) applied the distribution functions of snow cover and freezing depth of soil to snowmelt runoff analysis. Popov (1963) derived a general relationship for snowmelt runoff calculation using a distribution function of the retention storage over a basin. These results are widely used in long- and short-term runoff predictions.

To account for the effects of spatial variability on runoff, Koren and Kuchment (1971) developed a simple rainfall-runoff model based on a theoretic-probabilistic averaging of the point processes. A lack of spatial statistics of variables led them to assume most of the input data and parameters were normally distributed and only soil moisture capacity had exponential distribution. The importance of the spatial variability of soil hydraulic properties was shown by numerical analyses of rainfall-runoff processes on a hillslope assuming different hypothetical distributions and autocorrelation of the basin characteristics and rainfall (Freeze, 1979; Smith and Hebbert, 1979). Dagan and Bresler, (1983) analyzed infiltration processes depending on the spatial variability of hydraulic conductivity. Moore (1985) derived a spatially averaged rainfall-runoff equation using exponential distribution for both rainfall and infiltration capacity. Eagleson (1978) also used a derived probability distribution approach to illustrate how equations for spatially averaged infiltration and runoff could be developed

from point process considerations. The spatial distribution assumptions first used by Moore (1985) were later used by Schaake (1990) and Schaake and Liu (1989) in developing a simple monthly water balance model which is a precursor to some of the work reported below. A similar approach to parameterizing sub-grid processes was taken by Entekhabi and Eagleson (1989) who considered spatial variability in precipitation and soil moisture storage in a physically based context. Eagleson and Entekhabi ignored the effect of spatial variability in the hydraulic properties of the soil.

Water Storage Components

The land surface in SWB is represented with two layers. A thin upper layer consists of the vegetation canopy and the soil surface. A lower layer includes both the root zone of the vegetation and the ground water system. The root zone and the groundwater system are combined into a single layer to keep SWB as simple as possible. The SWB is being tested to determine if root zone and ground water components of the lower layer should be represented separately.

The amount of water that can be stored in each layer is limited. These limitations are model parameters. The storage state variable can be represented in terms of water content or in terms of water deficit. In SWB the storage state variable is soil moisture deficit only because moisture deficit may be useful in diagnosing model performance. In the spring in humid climates, moisture deficits are usually small so model moisture deficits would be small. Also soil moisture measurements are not adequate to estimate the water content of SWB over large areas because they are too scarce. Available soil moisture data can be used to test SWB, but because moisture deficit and moisture content are simply related, the moisture deficit variable is the state variable used in SWB.

The limits of moisture deficit are called maximum deficits, but these are equivalent in magnitude to maximum storage contents. The terms maximum deficit and water storage capacity are equivalent and can be used interchangeably. In humid climates where spring moisture deficits are low, the total moisture storage capacity can roughly be estimated from rainfall and runoff data

Water Balance of the Vegetation Canopy and Soil Surface

The upper layer is a short-term retention storage that principally represents the capacity of the vegetation canopy to hold water on the surface of the canopy. It also represents the capacity of the soil surface to store water in small depressions or in the top few millimeters of soil surface. The water balance of the upper layer is:

$$\frac{dD_u}{dt} = E_u - P + P_x \qquad (1)$$

where D_u is the moisture storage deficit in this layer. The maximum value of D_u is $D_{u,max}$ which also is the maximum storage capacity of the

upper layer. Inflow to the upper layer is from precipitation, P and all inflow will be retained until $D_{u,max}$ is filled (i.e., when D_u=0). Then excess inflow, P_x, becomes input into the lower layer. Water evaporates from the upper layer at the rate E_u.

Water Balance of Soil Moisture Storage (Lower Layer)

The lower layer is the main soil moisture storage reservoir. The water balance of this layer is:

$$\frac{dD_b}{dt} = E_b + Q_s + Q_g - P_x \qquad (2)$$

The moisture deficit in this layer is D_b. The maximum value of D_b is $D_{b,max}$ which also is the maximum water capacity of the lower layer. The value of $D_{b,max}$ depends mostly on the rooting depth and soil porosity. Runoff from the surface, Q_s and subsurface, Q_g and evapotranspiration, E_b, are outflows from the layer. All variables of Equations 1 and 2 are mean areal values.

Evapotranspiration

The upper layer is in close proximity to the atmosphere and contains water intercepted by leaves, stored in surface depressions or stored in top CM or so of the soil surface. This water evaporates locally at rates governed by the ability of the atmosphere to accept water. The lower layer includes the root zone of vegetation. Water is lost to the atmosphere from the lower layer by direct evaporation from the soil and by evapotranspiration through vegetation.

Evaporation from the Upper Layer

Water stored in this layer is distributed heterogeneously and partially over the area. Accordingly it is be possible for the average areal rate of evaporation, E_u, from this layer to be less than the potential rate even though local evaporation rates (e.g. from leaves) may exceed the areal average potential rate. It is assumed the effect of partial area coverage of upper layer moisture varies as a function of D_u and acts to decrease the actual areally averaged evaporation rate below the potential rate according to the relation:

$$E_u = E_p \left(1 - \frac{D_u}{D_{u,max}}\right) \qquad (3)$$

Evapotranspiration from the Lower Layer

Evapotranspiration from the lower layer, E_b, takes place only if evaporation from the upper layer is less than the potential rate. Accordingly the potential evaporation rate from the lower layer is reduced by the actual evaporation rate from the upper layer:

$$E_{pb} = E_p - E_u \qquad (4)$$

The actual evapotranspiration, E_b, is less than or equal to potential evapotranspiration, E_{pb}, as a function, $f(D_b)$, of the soil moisture deficit of the lower layer:

$$E_b = E_{pb} f(D_b) \tag{5}$$

The function $f(D_b)$ accounts for the effect of moisture stress on vegetation. Other forms of vegetation stress are neglected in SWB. A simple linear equation is used to estimate $f(D_b)$:

$$f(D_b) = 1 - \frac{D_b}{D_{b,max}} \tag{6}$$

Perhaps a more complex functional form for $f(D_b)$ may prove to be justified, but that would increase model complexity and would add at least one more model parameter. This should be investigated in future studies of how much complexity in the role of vegetation is justified, considering how the additional parameters would be estimated.

Equations 3 through 6 can be combined to form:

$$E_b = E_p \left(\frac{D_u}{D_{u,max}}\right)\left(1 - \frac{D_b}{D_{b,max}}\right) \tag{7}$$

The amount of evapotranspiration from the two layers can be estimated as:

$$E = E_p \left(1 - \left(\frac{D_u}{D_{u,max}}\right)\left(\frac{D_b}{D_{b,max}}\right)\right) \tag{8}$$

which is a nonlinear function of the soil moisture content of the both the upper and lower layers. A typical relationship of relative values of evapotranspiration, E/E_p and relative values of soil moisture deficit, D/D_{max}, ($D = D_u + D_b$ and $D_{max} = D_{u,max} + D_{b,max}$) is shown in Figure 1.

This evaporation scheme has been tested against observed evaporative flux measurements during the FIFE experiment (Mitchell, et al, this issue). SWB over-estimates evapotranspiration during wet periods of the FIFE experiment. A canopy resistance term was added to SWB as part of that study to remedy this problem. That canopy resistance term adds several additional parameters to SWB and is not included in the current study. Subsequent tests of SWB using rainfall and runoff data are planned with the canopy term included SWB and with some of the additional parameters estimated by remotely sensed vegetation measurements.

Subsurface Runoff

Subsurface runoff is assumed to be a linear function of the lower layer moisture content in excess of a minimum threshold, S_{max}:

$$Q_g = \begin{cases} Q_{max}\left(1 - \frac{D_b}{S_{max}}\right), & D_b < S_{max} \\ 0, & \text{otherwise} \end{cases} \qquad (9)$$

where Q_{max} is the potential subsurface runoff that occurs when the lower layer is saturated (i.e. when $D_b=0$). Equation (9) implies that the ground water system acts like a linear storage reservoir, a widely used hypothesis in hydrologic modeling. If there were no precipitation nor evaporation, the only outflow from storage would be an exponentially decreasing flow of subsurface runoff. The rate constant, Q_{max}/S_{max}, in this exponential function can be estimated from the recession portion of observed hydrographs. The value depends on topography, geology and soil hydraulic properties. When the lower layer moisture deficit, D_b, exceeds the threshold, S_{max}, subsurface runoff ceases. This allows the model to simulate ephemeral streams. Experience suggests that S_{max} is usually less than $D_{b,max}$.

It is important to note that water can leave the lower layer either as evapotranspiration or as subsurface runoff. In a sense these fluxes are in competition in the current version of SWB. Some competition between evapotranspiration and subsurface runoff is reasonable because riparian vegetation is sometimes more abundant that vegetation far from streams. On the other hand, much of the evapotranspiration is from an unsaturated root zone and unsaturated moisture in the root zone is not available for subsurface runoff. Perhaps the lower layer storage should be partitioned into root zone and groundwater layers. But this would increase model complexity and would add at least one parameter to govern the rate of percolation from the root layer to the ground water layer.

Surface Runoff and Infiltration

The supply of water to the lower zone is P_x, the excess of precipitation or throughfall from the upper layer. This water flux is available for surface runoff and infiltration into the lower layer. At the surface of the lower layer, some of P_x infiltrates into the lower layer; the excess becomes surface runoff.

The strategy taken in representing infiltration and surface runoff in SWB is first to consider the spatial variability of infiltration capacity. Because actual infiltration depends on precipitation as well as infiltration capacity, the spatial distribution of precipitation is considered next. Then the spatial distributions of infiltration capacity and precipitation are analyzed to derive equations for spatially averaged infiltration and runoff. These equations relate the spatially averaged runoff and infiltration to the spatially averaged infiltration capacity and precipitation. These equations are most appropriately applied to storm total accumulations. Finally a relationship is developed for the temporal variability of the spatially averaged infiltration capacity as a function of duration of accumulation.

Point Infiltration Capacity

Local rates of infiltration vary in space and time. At any time, the capacity of the soil to infiltrate water may exceed the actual infiltration rate if the supply of water to the surface does not keep the surface saturated. Temporal variability may be classified into variability during storm events and into changes in initial infiltration capacity between storm events.

At a point the flow of water into and within a vertical column of soil can be represented by the Richard's equation in the form:

$$\frac{\partial \theta}{\partial t} = \frac{\partial}{\partial z}\left[D(\theta)\frac{\partial \theta}{\partial z}\right] + \frac{\partial K(\theta)}{\partial z} \qquad (10)$$

where θ is the soil moisture content, $K(\theta)$ is the hydraulic conductivity and $D(\theta)$ is the soil water diffusivity which depends on the saturated hydraulic conductivity K_s. Philip (1969) developed an approximate solution to the Richards equation for the special case of infiltration with a uniform initial soil moisture state and saturated surface conditions. Philip's equation for the total cumulative volume of infiltration at a point is:

$$i_c(t) = St^{1/2} + Kt \qquad (11)$$

where K is close to the saturated hydraulic conductivity, K_s and S is sorptivity, a function of the diffusivity and the initial soil moisture state. Variable $i_c(t)$ denotes the cumulative volume of infiltration to time, t, assuming the surface remains saturated. This equation assumes an infinitely deep soil column so that water can percolate downward at a rate determined by the saturated hydraulic conductivity. In reality, the thickness of the soil column is finite. Therefore, the infiltration capacity is not necessarily limited by the saturated hydraulic conductivity of the soil, but by the available space to store water in the soil column and by the rate of lateral saturated subsurface flow in the hillslope toward the stream. Under natural conditions, precipitation does not support continuous saturated conditions at the soil surface (i.e. ponding), but a technique known as time compression analysis (TCA) (Sherman, 1943; Sivapalan and Milly, 1989; Salvucci and Entekhabi, 1994) can be used to adjust the time scale. TCA assumes that the maximum rate of infiltration (i.e. instantaneous infiltration capacity) during an event depends on the initial soil moisture condition and on the cumulative infiltration since the beginning of the event. The assumption that infiltration capacity depends on the current soil moisture state is used below to account for changes in infiltration capacity with time.

Spatial Variability of Infiltration Capacity

The spatial average rate of infiltration over a catchment during a time interval, $\triangle t$, is not well approximated by Philip's equation because of the heterogeneity of: initial moisture conditions, thickness of unsaturated soil column and soil hydraulic properties

(even if the soil type is essentially uniform). Also spatial variability in the depth of the soil column will lead to spatial variability of the time when the steady state infiltration rate becomes limited by lateral flux into the groundwater system. Considering the heterogeneity and complexity in space and time of the infiltration process, it is not clear if there is enough information available to derive systematically a simple set of equations for the spatially averaged infiltration rate. Therefore, an empirical approach guided by theoretical considerations is used to represent infiltration capacity in SWB. In a study of data from 52 infiltrometers placed in the 19.2 KM2 Guereb-Roriche catchment in northern Tunisia, Berndtsson (1987) approximated the time decay of infiltration with Horton and Philips infiltration functions. Bendtsson found that the parameters of these functions varied spatially, but the spatial coefficient of variation of all of the parameters and of the cumulative amounts of infiltration was close to 1.0. This suggests that an exponential distribution might be used to account for the effects of spatially distributed point infiltration capacities for a fixed time interval. Loague and Gander (1990), reported infiltration results for a small 0.1 KM2 rangeland experimental watershed, (R-5), in the Little Washita Experimental Watershed of the U.S. Agricultural Research Service. A total of 157 infiltrometer measurements were made on a 25 M grid over a period of about 2 months. There is not much of a trend to the average of the measurements over time. The coefficient of variation of this full set of measurements is 0.73. They concluded a lognormal distribution gave a better fit to the data than a normal distribution. They attempted to create a map showing the spatial distribution of the infiltration capacity, but they concluded that the spatial decorrelation distance was shorter than 25 M. Moreover, the catchment has a nearly uniform soil so they conclude that the spatial variability of the infiltration results cannot be explained by soil texture. Presumably the variability of the infiltration results was caused by variability of soil hydraulic properties and by variability of point soil moisture content. It is possible that the best spatial distribution of infiltration capacity is a function of space scale. The authors are not aware of infiltration studies at scales larger that 19.2 KM2. It seems reasonable to assume the coefficient of variation of the spatial distribution of infiltration capacity might increase with area because of more sources of heterogeneity. In view of the limited infiltration data available at the scale at which SWB would be applied, an exponential distribution of infiltration capacities is assumed:

$$f(i_c)=(\frac{1}{I_c})\exp[-\frac{i_c}{I_c}] \qquad (12)$$

where i_c is the point infiltration capacity during a storm event and I_c is the spatially averaged infiltration capacity. If another distribution were used, a procedure would be needed to account for the spatial coefficient of variation of the infiltration capacity. In view of the information available and the need to keep SWB as simple as possible additional complexity does not seem justified. Future work should be conducted to examine the sensitivity of SWB to other distribution forms that might be considered. Note that

Equation (12) applies to the total capacity of infiltration during a storm event. The actual amount of infiltration depends on the spatial distribution of both the infiltration capacity and the precipitation excess, P_x, during the storm.

Precipitation

The spatial distribution of precipitation is highly variable and depends on the magnitude of the precipitation event. Extensive gage measurements of thunderstorm rainfall in the 20,000 KM2 Muskingum, OH river basin were made as part of a WPA project in the late 1930's. The average gage density over this large area was better than 1 gage per 50 KM2. These data showed that the spatial coefficient of variation of precipitation is smaller for the larger storms (Hydrometerological Section, 1945). The spatial coefficient of variation also tends to increase with area. Analysis of data for the maximum 6 hour period of 38 storms gave the following relationship for the spatial coefficient of variation:

$$C_v = 2.58 P^{-1.56} A^{0.20} \qquad (13)$$

where P is the areal average precipitation [CM] and A is the area [1000's KM2]. Equation (13) suggests the median coefficient of variation for a 1 CM (10 MM) event over a 20,000 KM2 area would be 2.96, but for a 2.5 CM event this would be only 0.71. The coefficient of variation of individual events in the Muskingum basin was highly variable and fell in a multiplicative range of .65 to 1.55 times the coefficient of variation given by Equation (13). The spatial coefficient of variation of precipitation also decreases with increasing time duration of the precipitation. Other investigators have shown that an exponential distribution function can often be used to account for spatial variability of rainfall for small areas (Moore, 1991; Koren, 1993). As an example, Figure 2 displays distribution functions of relative values of precipitation, $K_p = p/P$ obtained by radar measurements for a small experimental basin, about 40 KM2, in the USSR (Koren, 1993). A theoretical justification of the exponential distribution of rainfall under some assumptions was given by Vinogradov (1988). These relationships apply to the rainy portion of the area. The fractional coverage of the area is also a factor to be considered. Daily precipitation data for 40 years were studied in a 90,000 KM2 rectangle centered on Lamont, OK. The average coefficient of variation in the rainy area ranged from 1.1 to 1.3, depending on the month. The average rainy proportion of the area was between 0.43 and 0.66 with a standard deviation of about 0.25 for individual events. The fraction of the area with rain was positively correlated with the average rain over the total area. Below a scale of about 10,000 KM2, the effect of partial area coverage for total storm precipitation should not be very important for daily or longer time periods and for significant rain events. Beyond about 10,000 KM2 partial area coverage of precipitation may become so important that it should not be neglected by SWB. Future work is needed to see how best to include the effect of partial area of coverage of rain in SWB for areas greater than about 10000 KM2. Although it is recognized the spatial coefficient of variation of rainfall is highly variable from event to event, it is assumed here

that the spatial distribution of precipitation is given by:

$$f(p)=\frac{1}{P}\exp[-\frac{p}{P}] \tag{14}$$

where p is the storm total precipitation at a point and P is the spatially averaged storm total precipitation. It is assumed that the distribution of P also applies to P_x because the storage capacity of the upper layer is small. It would be desirable in future studies to investigate a more complex spatial distribution of precipitation to consider the effect of temporally varying coefficient of variation of precipitation. If SWB is applied using observed precipitation forcing this is not a significant problem because the spatial distribution of precipitation can be estimated from observations, especially for large areas. But if SWB is used within an atmospheric model, some method to estimate both the spatial coefficient of variation of rain in rainy areas and the fraction of rainy area is needed.

Derived Distribution for Actual Infiltration and Storm Total Surface Runoff

Assume that at a point during a storm that the total amount of water that would infiltrate would be equal to the precipitation amount at that point if the precipitation were less than or equal to the infiltration capacity. This neglects the possibility that instantaneous precipitation rates during the storm might exceed the instantaneous infiltration capacity. Accordingly the point amount of surface runoff would be:

$$q_s=\begin{cases} p_x-i_c\ , & p_x>i_c \\ 0\ , & \text{otherwise} \end{cases} \tag{15}$$

Because p_x and i_c are spatially distributed random variables, q_s also is a spatially distributed random variable. Accordingly the average surface runoff from the area is:

$$Q_s=\int_0^\infty q_s f(q_s)\,dq_s \tag{16}$$

where $f(q_s)$ is the derived distribution function of surface runoff. The density function for $f(q_s)$ depends on the joint distribution of p_x and i_c. Since p_x and i_c apply to an entire storm period, it is reasonable to assume the spatial distribution of precipitation is independent of the initial state of the catchment and therefore of i_c. Thus

$$f(p_x,i_c)=f(p_x)f(i_c) \tag{17}$$

The cumulative distribution function for q_s is:

$$F(q_s\le Q_s)=\int_{R(q_s\le Q_s)}\int f(p)f(i_c)\,di_c\,dp \tag{18}$$

where $R(q_s \leq Q_s)$ is the region of the (p, i_c) plane where q_s is less or equal to Q_s. Integration of Equation (18) gives:

$$F(q_s) = \frac{I_c}{P_x + I_c} \exp\left[-\frac{q_s}{P_x}\right] \tag{19}$$

The density function for q_s has a finite probability that $q_s = 0$:

$$F(q_s = 0) = \frac{I_c}{P_x + I_c} \tag{20}$$

The density function is:

$$f(q_s) = \frac{I_c}{P_x + I_c} \delta(0) + \frac{P_x}{P_x + I_c} \exp\left[-\frac{q_s}{P_x}\right] \tag{21}$$

where $\delta(0)$ is the Dirac delta function. It follows that the average value of q_s is:

$$Q_s = \frac{P_x^2}{(P_x + I_c)} \tag{22}$$

This equation was originally derived by Moore (1985) and it is essentially the same as the so-called SCS curve number equation (SCS, 1972). The precipitation input to the lower layer, P_x, is divided into surface runoff and infiltration:

$$P_x = Q_s + I \tag{23}$$

so, the spatially averaged actual infiltration, by combining Equations 22 and 23 is:

$$I = \frac{P_x I_c}{P_x + I_c} \tag{24}$$

Infiltration and Surface Runoff During a Finite Time Interval

SWB is a continuous model that must operate in time steps, $\triangle t$. Model time steps within an atmospheric model may be only a few minutes. Therefore, SWB must estimate how the infiltration and surface runoff processes operate during finite intervals within a storm event. To do this it is assumed that I_c is a function of the duration of the time step, $\triangle t$. Also an assumption similar to the TCA assumption is made that I_c depends on the current moisture state. During a storm event, the initial condition important for infiltration is the soil moisture in the upper portion of the soil. During and between

storms, infiltrated water percolates and plant roots extract water from the wettest portions of the soil profile. These processes tend to redistribute water in the soil column so that the initial soil moisture near the surface tends to be correlated with the average soil moisture integrated over the entire soil column. Duan et al (1995, this issue) found that during the FIFE experiment the spatially averaged total soil moisture measured in the top ten CM over the entire FIFE area (15 KM by 15 KM) was well correlated with the total soil moisture in the top two meters. This suggests that D_b is correlated with the initial moisture conditions that influence the infiltration process (i.e. D_b is correlated with I_c). For long time steps of many days to a month, it may be reasonable to substitute D_b for I_c. But for time steps, $\triangle t$, less than a typical storm duration, I_c is less than D_b. Therefore it is assumed that

$$I_{c,i}(\Delta t)=\phi(\Delta t)D_{b,i-1} \tag{25}$$

The cumulative infiltration capacity, $I_{c,i}(\triangle t)$, during the interval $(i-1)\triangle t<t<i\triangle t$ increases with $\triangle t$, but the rate of increase diminishes as $\triangle t$ increases. Because $I_{c,i}$ is a spatially averaged variable of a nonlinear and heterogenous process, point infiltration equations do not apply. A number of alternative expressions for $\phi(\Delta t)$ were considered, subject to the following condition. If the actual infiltration $I_i(\triangle t)$ were equal to the infiltration capacity, $I_{c,i}(\triangle t)$, then

$$D_{b,i}=D_{b,i-1}-I_{c,i}(\Delta t) \tag{26}$$

so that

$$D_{b,i}=D_{b,i-1}(1-\phi(\Delta t)) \tag{27}$$

similarly

$$D_{b,i-1+n)}=D_{i-1}(1-\phi(\Delta t))^n \tag{28}$$

But consistency for an arbitrary value of $\triangle t$ requires

$$D_{b,i-1+n}=D_{i-1}-I_{c,i}(n\Delta t) \tag{29}$$

Since

$$I_{c,i}(n\Delta t)=d_{i-1}\phi(n\Delta t) \tag{30}$$

it follows that

$$D_{b,i-1+n}=D_{i-1}(1-\phi(n\Delta t)) \tag{31}$$

This requires

$$(1-\phi(n\Delta t))=(1-\phi(\Delta t))^n \tag{32}$$

which is satisfied if

$$\phi(\Delta t)=1-\exp(-K_{dt}\Delta t) \quad (33)$$

Therefore the current value of I_c is:

$$I_c=D_b(1-\exp(-K_{dt}\Delta t)) \quad (34)$$

Model Evaluation and Testing

SWB is tested using historical data from three basins in the United States, representing different climatological conditions. The performance of SWB is compared with that of three other hydrologic models, including one operational hydrologic forecast model and two land surface process parameterizations of atmospheric models. The results of an investigation into the model's ability to handle different time steps is presented. This includes tests to understand the limitations of SWB to handle time steps different from the time step for which SWB parameters were calibrated.

Tests of SWB for Selected Basins in the United States

SWB was tested using observations for three different basins in the United States. The three basins chosen for this study are Bird Creek at Sperry in Oklahoma, Leaf River near Collins in Mississippi and the French Broad at Rosman in North Carolina. These basins are well studied and documented basins (see WMO 1975; Brazil 1988). They have distinct hydrologic characteristics, representing respectively, dry, moderate and humid regions. Hydrologic data ranging from 7 to 18 years were collected from these basins. Table 1 lists information about the three basins. Three measures of performance were used in the tests: the daily root mean square difference (DRMS) between simulated and observed daily flows, the monthly volume root mean square error (MVRMS) and the coefficient of efficiency (E). The DRMS statistic was used to test how well the model simulated daily flow fluctuations. It is computed as

$$DRMS=\sqrt{\frac{\sum_{i=1}^{N}(q_{s,i}-q_{o,i})^2}{N}} \quad (35)$$

where $q_{s,i}$ and $q_{o,i}$ denote the simulated and observed daily streamflow discharge, respectively, I indicates the day and N is the total number of days in the period. In computing the objective function value, a warm-up period of 5 months was used to reduce the uncertainty caused by unknown initial conditions. The MVRMS measures the error between the estimated and observed monthly water volume. This statistic is a very useful statistic to test how well the long term water budget is represented. The MVRMS is defined as:

$$MVRMS=\sqrt{\frac{\sum_{i=1}^{M}(y_{s,i}-y_{o,i})^2}{M}} \quad (36)$$

where $y_{s,i}$ and $y_{o,i}$ denote the simulated and observed monthly runoff, respectively, I indicates the month and M is the total number of months in the period. The coefficient of efficiency, E, indicates the degree of association between the observed and simulated flows (Nash and Sutcliffe, 1970). E is defined as:

$$E=\frac{\sum_{i=1}^{N}(q_{o,i}-\overline{q_o})^2-\sum_{i=1}^{N}(q_{s,i}-q_{o,i})^2}{\sum_{i=1}^{N}(q_{o,i}-\overline{q_o})^2} \quad (37)$$

where q_o is the mean daily observed streamflow discharge.

Calibration of SWB

SWB was first calibrated to the three basins using historical data ranging from 5 years to 9 years. The time scale at which the model was run was 6 hours, using 6 hourly precipitation data. A unit hydrograph was used in combination with SWB to route the runoff generated from SWB into streamflow discharge values at stream gage. The unit hydrograph used here was a synthetic unit hydrograph based on a two-parameter Gamma function (Nash, 1959). An automatic calibration procedure known as the Shuffled Complex Evolution (SCE-UA) method developed by Duan et al. (Duan et al., 1992 and 1994) was used to estimate the model parameters. The objective function used was the MVRMS statistic. The MVRMS was chosen for calibration to assure the model represented the long term water balance and because calibration tests using the DRMS statistic led to large biases in monthly runoff simulations. A major issue in model calibration is to specify quantitatively what the calibration is to achieve (Brazil, 1988). Further study is needed to determine the best automatic calibration procedures for SWB. Perhaps it would be better to use a weighted combination of MVRMS and DRMS with most of the weight on MVRMS to assure unbiased long term results. This should select parameters that give the best daily performance from among those that give good water balances. After the model parameters were determined for each basin, SWB was verified using independent historical data ranging from 2 years to 9 years. The purpose of the verification runs is to check whether the calibrated model performs consistently during and beyond the calibration period.

Table 2 summarizes the calibration as well as the verification statistics for SWB (see rows for SWB model type). The results suggest that the DRMS and MVRMS statistics are generally better for calibration periods than for the verification periods. There are two probable explanations for this difference. First the model parameters were tuned to the calibration data. Thus it is expected

that model should perform better during the calibration period, although this difference should not be too big. The second explanation for the performance discrepancies is that the hydrologic conditions were different between the calibration and verification periods.

Table 3 lists the annual hydrologic variables for the three basins during the calibration and verification periods. Note that for all three basins, the annual streamflow discharges were higher for the verification periods than for the calibration periods. Higher DRMS and MVRMS statistics are expected for periods with higher streamflow discharge. Thus the magnitude of the streamflow discharges was partially responsible for the poorer statistics in the verification periods. The E statistics seem to support this argument. Note that the E values for the verification periods are comparable to that of the calibration period except for the Bird Creek. For the Bird Creek basin, another factor contributed to the poorer statistics in the verification period. Only 5 years of historical data were used to calibrate the model and the 5 years happened to be relatively dry. Thus the parameters obtained from calibration may not be representative of the basin. Time series plots of the observed and simulated monthly runoff (Figures 3-a to 3-c) indicate simulated and observed monthly average discharges generally agree. Figures 4-a to 4-c are the x-y plots of the observed and simulated daily streamflow discharges. Observed and simulated daily values match each other very well, except a few cases which fall outside the one standard deviation range. Better results may be possible by giving some weight to the DRMS statistic in the calibration objective function. Also including more high flow years in the Leaf river calibration period may help to improve the underestimation of the largest flows.

Comparison of SWB with SAC-SMA, the OSU Model and the Manabe Bucket Model

Three other hydrologic models are selected for intercomparison with SWB. These are the Sacramento Soil Moisture Accounting (SAC-SMA) model, a soil hydrology model developed at Oregon State University (OSU) and the Manabe Bucket model. SAC-SMA was originally developed by Burnash et al in 1973 (Burnash et al., 1973). SAC-SMA represents spatially averaged hydrologic processes and there are strong physical arguments to support the model. It has 6 state variables and 16 parameters, not counting the 12 parameters used for adjusting potential evaporation values. Of the 16 parameters, 13 need to be determined by calibration. For a detailed description of SAC-SMA, see Burnash et al. (1973), Peck (1976) and Brazil (1988). The SAC-SMA model was calibrated to the three basins in the same way as SWB as described in the previous section. After the calibration was completed, verification runs were conducted using historical data not included in the calibration period. The results for SAC-SMA (Table 2) gave the same tendency as SWB. That is, the calibration statistics were better than the verification statistics. The same explanations given for SWB can also be used for SAC-SMA results. The second model compared is the soil hydrology model developed by Mahrt and Pan (1984), which was used as the land surface hydrologic parameterization in the Oregon State University One-Dimensional Planetary Boundary Layer (OSU 1-D PBL) model (Ek and Mahrt, 1991).

This soil hydrology model is refer to as the OSU model. For a detailed discussion of the OSU model, see Mahrt and Pan (1984) and Pan and Mahrt (1987). The OSU model is based on the finite difference solution to the one-dimensional Richards Equation (Hillel, 1980). It contains two soil layers: a thin upper layer of 5 centimeters and a thick lower layer of 95 centimeters. The OSU model explicitly accounts for the effect of vegetation on evapotranspiration by inclusion of the canopy layer. However it does not account for the spatial variability in hydrologic variables. To account for the effect of spatial heterogeneity, the infiltration formulation in the OSU model was replaced by the infiltration formulation in SWB. A unit hydrograph was also used to route the runoff generated from the OSU model into streamflow discharge values at stream gage.

Most of the parameters in the OSU model were derived using the soil and vegetation information. Four of the OSU model parameters are considered important in the rainfall/runoff calculation. These parameters are the hydraulic conductivity, hydraulic diffusivity, the root depth and the parameter controlling the infiltration. The four parameters were calibrated to three basins using the same procedures described previously. Because the OSU model was designed for small time step simulations, an hourly time step was used in this case. An assumption was made that rainfall was evenly distributed over every six hour period. The calibration and verification results are also presented in Table 2. Runoff simulation from the OSU model without calibration of these four parameters was not very good. Tests of the original OSU model without the SWB infiltration parameterization were not made. Overall, the error statistics for the OSU model are comparable to the error statistics for SWB and SAC-SMA for the Bird Creek and the Leaf River basins. Poorer results were obtained for the French Broad River basin. The main reason for the poorer results in this basin may be that the sub-surface runoff component is the major contributor of the total runoff. The OSU model does not have a subsurface runoff component. Calibration results also point out that the root depth is a very important parameter in controlling runoff generation and this parameter was not calibrated in the OSU model tests. The variation of its value from basin to basin agrees with the variation of the D_{max} parameter in the SWB model.

The Manabe Bucket model (Manabe, 1969) - was also tested. The Manabe Bucket model has been widely used as the land surface parameterization in many GCM-type models and operational mesoscale atmospheric models like the Eta model in the NMC (WCRP, 1993; Mitchell, 1994). This model is extremely simple with just one adjustable parameter, i.e., the depth of the bucket. A fixed depth is normally assumed everywhere the model is used. In this study a fixed depth of 150 millimeters was assumed for all three basins. The Manabe Bucket was used on the three basins and the statistics were computed for the calibration and verification periods. The results are recorded in Table 2. Additional tests were made to optimize the bucket depth. However the improvements in the statistics were marginal. Statistics in Table 2 indicate that Manabe Bucket model performed substantially worse than the other three models. Judging from the statistics, the Manabe Bucket model is not useful at all from a hydrologic forecast point-of-view. The negative values in E

statistic imply that the Manabe Bucket runoff estimates were not even as good as the long term average of runoff value.

The OSU model gave somewhat poorer runoff simulation compared to SWB and SAC-SMA. The strength of the OSU model is in the calculation of evapotranspiration. However there were no observed data available to compare evapotranspiration simulation results in this study. Detailed tests of the OSU model and the SWB model using data from the First International Satellite Land Surface Climatology Project (ISLSCP) Field Experiment (FIFE) have been made by Mitchell et al (this issue).

A comparison of the performance of SWB with SAC-SMA shows that SAC-SMA generally performs better than SWB. This is not surprising considering that the SAC-SMA model is more complicated than the SWB model. The difference between the two models is smaller in the verification periods. Comparing the time series plots of the observed and simulated monthly runoff for SAC-SMA (Figures 5-a to 5-c) with that for SWB (Figures 3-a to 3-c) suggests that both models produced similar results.

Tests of SWB Sensitivity to $\triangle t$

SWB explicitly accounts for the effect of time scaling on the relationships among hydrologic variables. It is designed to operate for a range of values of $\triangle t$ from a few minutes to a few days. Results of runoff simulations for Bird Creek (Oklahoma, USA) were used to test the sensitivity of model performance to the choice of $\triangle t$. One approach, is to test if the model performs the same for different values of $\triangle t$ when model parameters are held constant. Another approach is to test if model calibration with different values of $\triangle t$ leads to the same model parameters. Calibrations of SWB for bird Creek yielded almost constant parameters over substantial ranges of $\triangle t$ as shown in Table 4. Parameter values are most consistent for $\triangle t$ up to one day. Parameters for $\triangle t$ = 4 days are quite different from parameters for shorter time steps. Corresponding values of the performance statistics are given in Table 5. The performance of daily statistics degrades substantially beyond one day. The monthly performance begins to degrade substantially after 2 days. Table 5 shows that SWB performed slightly better when calibrated and operated at a 1 day time step than at a 6 hour time step. This could be because of limitations of the parameterizations in SWB or because of interaction between the non-linear functions in SWB and sampling noise in the 6 hour data.

Because SWB was designed to operate over a range of time steps and because there is some variability in the parameters with $\triangle t$ in Table 4; simulations of SWB using different values of $\triangle t$ and different sets of parameters were made.

The first set of tests was to use parameters calibrated for one time step in simulations over a range of time steps. Table 6 gives performance statistics for simulations operated over a range of time steps using parameters calibrated at a one-day time step. Table 7 gives results for the same simulations as Table 6, but using parameters calibrated at 6 hour $\triangle t$ using actual 6 hour precipitation.

Clearly, SWB performance decreases if it is operated at a different Δt than used in calibration, but performance is reasonably robust in that simulations at 12 hour Δt can be done relatively well with parameters calibrated at either 6 hours or 1 day. The results in Tables 6 and 7 have important implications for coupled atmosphere/land surface model applications. It is not surprising that the performance results in Tables 6 and 7 show that SWB works best at the time step for which it is calibrated. But it is surprising, that the performance is so sensitive between 6 hour and 24 hour intervals when the same parameters are used. This is surprising because the 6 hour and 24 hour parameter sets in Table 4 are not very different. Since many atmospheric models operate at time steps less than 1 hour, additional tests should be made using 1 hour precipitation data. This also means that 1 hour precipitation data are important for hydrologic model development and testing. It is even more important however that very similar values of model parameters give different performance when the model is operated at the same time step. This is important because parameters used in atmospheric models must be estimated a priori, without calibration; although calibrated parameters might be used to develop a priori parameter estimation techniques. This means that the sensitivity of model performance to uncertainty in a priori parameter estimation procedures should be thoroughly investigated. A second set of tests was made to study the effect of temporal averaging of precipitation on model performance. SWB was operated at different time steps, up to 1 day with uniform daily rainfall applied for each time step. Test results using parameters calibrated with actual precipitation at daily and 6 hour time steps are given in Tables 8 and 9, respectively. The 6 hour parameter set used for Table 9 is the same as for Table 7 and is based on 6 hour precipitation forcing. A notable result in these Tables is that the 6 hour performance when daily parameters are used is much better when the actual 6 hour rainfall is used as input (Table 7) than if daily average rain is used (Table 9). A similar result applies to the 12 hour time step. In each case, it is better to use 6 hour rather than daily parameters for simulations up to 12 hours. It is interesting to note also that the best performance was for 12 hour Δt when 6 hour parameters were used. In general the best performance shifted toward simulations with Δt closer to the 1 day period over which the precipitation was averaged. A third set of tests was made using uniform daily precipitation. For these, parameters were calibrated for a 6 hour Δt and uniform daily precipitation. These parameters were then used for simulations over a range of Δt and the results are given in Table 10. This improved the 6 hour uniform rain simulations over those obtained in Table 9. Together the results in Tables 9 and 10 show that model performance is highly sensitive both to Δt used for simulation and calibration when the model is forced with uniform daily precipitation.

The combined results of the time step tests in Tables 6-10 suggest the obvious conclusion that SWB should be calibrated at a value of Δt as close as possible to the value of Δt to be used in the application. It is also better to use actual precipitation for the same Δt used in simulation, even if the parameters were calibrated for a different Δt. Finally if the only precipitation data available is daily, then model performance cannot be improved by operating at a

time step less than 1 day. But if the model is to be operated at a smaller time step as part of another model, then the performance can be improved by calibrating the parameters at the time step the model is to be operated.

Summary

A simple water balance (SWB) model was developed that takes into account spatial variability of inputs and soil moisture capacity. The probability distributions of spatial processes were used to upscale local processes to large scale. Exponential distributions of precipitation and infiltration capacity led to nonlinear equations for surface runoff and infiltration.

The SWB model can be regarded as a bucket model with conceptually defined physics of surface processes. The model does not account explicitly for vegetation dynamics, but options to do this are being developed and tested. It is assumed that subgrid variation is more important for water budget than for energy budget calculations and that potential evaporation can be used as a surrogate for energy forcing.

The SWB model gave results comparable with other models that have more complex representations of surface runoff processes and the effects of vegetation on evapotranspiration. This may partly have occurred because all of the models were applied using the same calibration criteria. If other information had been used (such as vegetation information from remote sensing), the more complex models may have performed much better than SWB. On the other hand such additional information could be used to support SWB parameters as well. There is a temptation to add more complexity to SWB to compensate for its obvious limitations but the purpose of SWB is to remain as simple as possible. It is easier to err on the side of having too much complexity (given the data available) than too little.

For the coupling of atmospheric and hydrological models it is very important to consider the temporal scaling. Hydrological models usually deal with the larger time steps than atmospheric models. The SWB model was formulated to operate at any time step up to about 24 hours.

SWB Model Summary

The land surface in SWB is represented with two layers. A thin upper layer consists of the vegetation canopy and the soil surface. A lower layer includes both the root zone of the vegetation and the ground water system. The root zone and the groundwater system are combined into a single layer to keep SWB as simple as possible. The upper layer is a short-term retention storage that principally represents the capacity of the vegetation canopy to hold water on the surface of the canopy. It also represents the capacity of the soil surface to store water in small depressions or in the top few millimeters of soil surface. The moisture storage deficit in this

layer is D_u. The maximum value of D_u is $D_{u,max}$ which also is the maximum storage capacity of the upper layer. Inflow to this upper layer is from precipitation, P and all inflow will be retained until $D_{u,max}$ is filled (D_u=0). Then excess inflow, P_x, becomes input into the lower layer. Water evaporates from the upper layer at the rate E_u which is the rate of potential evaporation. The resulting balance is:

$$\frac{dD_u}{dt} = E_u - P + P_x \tag{38}$$

The upper layer is a short-term retention storage that principally represents the capacity of the vegetation canopy to hold water on the surface of the canopy. The moisture storage deficit in this layer is D_u. The maximum value of D_u is $D_{u,max}$ which also is the maximum storage capacity of the upper layer. Inflow to this upper layer is from precipitation, P and all inflow will be retained until $D_{u,max}$ is filled (D_u=0). Then excess inflow, P_x, becomes input into the lower layer. Water evaporates from the upper layer at the rate E_u which is the rate of potential evaporation. The resulting balance is:

$$\frac{dD_u}{dt} = E_u - P + P_x \tag{39}$$

The average areal rate of evaporation, E_u, from this layer is estimated as:

$$E_u = E_p \exp\left\{-\frac{D_u}{D_{u,max}}\right\} \tag{40}$$

The actual evapotranspiration, E_b, from the lower layer is computed as:

$$E_b = E_p\left[1 - \frac{D_b}{D_{b,max}}\left(1 - \exp\left\{-\frac{D_u}{D_{u,max}}\right\}\right)\right] \tag{41}$$

which is a nonlinear function of the soil moisture content of the both the upper and lower layers. A typical relationship of relative values of evapotranspiration, E/E_p and relative values of soil moisture deficit, D/D_{max}, ($D = D_u + D_b$ and $D_{max} = D_{u,max} + D_{b,max}$) is shown in Figure 1.

Subsurface runoff is assumed to be a linear function of the lower layer moisture content in excess of a minimum threshold, S_{max}:

$$Q_g = \begin{cases} Q_{max}\left(1 - \frac{D_b}{S_{max}}\right), & D_b < S_{max} \\ 0, & \text{otherwise} \end{cases} \tag{42}$$

where Q_{max} is the potential subsurface runoff that occurs when the

lower layer is saturated (i.e. when $D_b=0$). Surface runoff is computed as:

$$Q_s=\frac{P_x^2}{(P_x+I_c)} \quad (43)$$

where I_c is:

$$I_c=D_b(1-\exp(-K_{dt}\Delta t)) \quad (44)$$

Summary of SWB Model Parameters

SWB has five parameters:

$D_{b,max}$ = Lower layer maximum soil moisture deficit (also maximum moisture content) (units of MM)

$D_{u,max}$ = Upper layer maximum moisture deficit (also maximum moisture content) (units of MM)

S_{max} = Threshold lower layer moisture deficit; ground water runoff ceases when the lower layer deficit exceeds this value (units of MM)

Q_{max} = Maximum potential ground water runoff rate (units of MM/day)

K_{dt} = Infiltration capacity scale parameter (units of day^{-1})

SWB has two state variables:

D_u = Moisture deficit in the upper layer (units of MM)

D_b = Moisture deficit in the lower layer (units of MM)

References

Anderson E. A., 1984. Inclusion of frozen ground effects in a flood forecasting model, Paper presented at the Fifth Northern Research Basins Symposium and Workshop, March 19-23, 1984, Vierumaki, Finland, 12p.

Avissar, R. and H. M. Verstraete, 1990. The representation of continental surface processes in atmospheric models. Rev. Geophys., 28, 35-52.

Berndtsson, R., 1987. Application of infiltration equations to a catchment with large spatial variability in infiltration. Hydr. Sci. J., 32(3), 399-413.

Brazil, L. E., 1988. Multilevel calibration strategy for complex hydrologic simulation models. Ph.D. Thesis, Department of Civil Engineering, Colorado State University, Fort Collins.

Burnash, R.J.C., R.L. Ferral and R.A. Maguire, 1973, A generalized streamflow simulation system: conceptual models for digital computers, Joint Federal-State River Forecast Center, Sacramento, California, 1973.

Carson, D. J., 1982. Current parameterizations of land-surface processes in atmospheric general circulation models. Land Surface Processes in Atmospheric General Circulation Models, P.S. Eagleson, Ed., C. U. P., 67-108.

Chen, Z.-Q., R. S. Govindaraju and M. L. Kavvas, 1994. Spatial averaging of unsaturated flow equations under infiltration conditions over areally heterogeneous fields, 1. Development of models, Water Resour. Res., 30(2), 523-533.

Dagan, G. and E. Bresler, 1983. Unsaturated flow in spatially variable fields, 1. Derivation of models of infiltration and redistribution, Water Resour. Res., 19(2), 413-420.

Dickinson, R. E., A. Henderson-Sellers and P. J. Kennedy, 1993. Biosphere-Atmosphere Transfer Scheme (BATS) Version 1e as coupled to the NCAR Community Climate Model, Tech. Note TH-387+STR, Natl. Cent. for Atmos. Res., Boulder, Colorado.

Duan, Q., Sorooshian, S. and Gupta, V. K., 1992. Effective and efficient global optimization for conceptual rainfall-runoff models. Water Resour. Res., 28(4), 1015-1031.

Duan, Q., Sorooshian, S. and Gupta, V. K., 1994. Optimal use of the SCE-UA global optimization method for calibrating watershed models. J. of Hydr., 158, 265-284.

Eagleson, P. S., 1972. Dynamics of flood frequency. Water Resour. Res., 8(4), 878-898.

Eagleson, P. S., 1978. Climate, Soil and Vegetation, 5. A Derived Distribution of Storm Surface Runoff. Water Resour. Res., 14(5), 741-748.

Ek, M. and L. Mahrt, 1991, OSU 1-D PBL model user's guide, College of Oceanic and Atmospheric Sciences, Oregon State University, Corvallis, Oregon.

Entekhabi, D. and P. S. Eagleson, 1989. Land surface hydrology parameterization for atmospheric general circulation models including subgrid scale spatial variability. J. Clim., 2, 816-831.

Famiglietti, J. S. and E. F. Wood, 1994. Multiscale modeling of spatially variable water and energy balance processes, Water Resour. Res., 30(11), 3061-3078.

Freeze, R. A., 1980. A stochastic-conceptual analysis of rainfall-runoff processes on a hillslope. Water Resour. Res., 16(2), 398-408.

Greminger, P. J.,Y. K. Sud and D.R. Nielsen, 1985. Spatial variability of field measured soil-water characteristics. Soil Sci.

Soc. Am. J., 49(5), 1075-1082.

Komarov, V. D., 1959, Snowmelt runoff of the lowland rivers of Europe of the USSR, Gidrometeoizdat, Moscow (in Russian).

Hillel, D., 1980, Fundamentals of soil physics, Academic Press, New York.

Hydrometeorological Section, 1945, Thunderstorm Rainfall Part 1: Text, Hydrometeorological Report No. 5. U.S. Weather Bureau

Jakeman, A.J. and G.M. Hornberger, 1993, How much complexity is warranted in a rainfall-runoff model?, Water Resour. Res, 29(8), 2637-2649.

Jakeman, A.M. and G.M. Hornberger, 1994, Reply (Paper 94WR01805), Water Resour. Res., 30(12), 3567.

Mahrt, L. and H.-L. Pan, 1984, A two-layer model for soil hydrology, Bound.-Layer Meteorol., 29, 1-20.

Manabe, S., 1969, Climate and ocean circulation. I: The atmospheric circulation and the hydrology of the earth's surface, Mon. Wea. Rev., 97, 739-774.

Mitchell, K.E., 1994, GCIP initiatives in operational mesoscale modeling and data assimilation at NMC, Preprint, AMS Fifth Conference on Global Change Studies, Nashville, TN, 23-28 January.

Mitchell, K.E., F. Chen, J. Schaake, Y. Xue, H.-L. Pan, V. Koren, Q. Duan and A. Betts, 1995, Modeling of land-surface evaporation by four schemes and comparison with FIFE observations, Journal of Geophysical Research, this issue.

Koren, V. I., Kuchment, L. S., 1971. A mathematical model of rain flood formation, optimization of its parameters and use in hydrological forecasting, Meteorology and Hydrology, 11, 59-68, (in Russian).

Koren, V. I., 1991. Mathematical modeling and forecasting of river runoff, Gidrometeoizdat, Leningrad, USSR, (in Russian).

Koren, V., 1993. The potential for improving lumped parameter models using remotely sensed data, Proceedings of the 13th Conference on Weather Analysis and Forecasting, August 2-6, 1993, Vienna, VA, USA, 397-400.

Lavel, K., 1988. Land surface processes. In M. E. Schlesinger (ed), Physically-based Modeling and Simulation of Climate and Climate change - part 1, Klumer academic Publ., 285-306.

Moore, R. J., 1985. The probability-distributed principle and runoff production at point and basin scales, Hydrological Sciences Journal, 30(2), 273-297.

Moore, R. J., D. M. Cooper, R. J. Harding, G. Roberts and A. Calver,

1991. Large-scale Hydrological Modeling: a Systems Analysis, Institute of Hydrology, Wallingford, Oxon, X10 8BB.

Nash, J. E., 1959, Systematic determination of unit hydrograph parameters, J. Geophysical Res., 64, 111-115.

Nash, J. E. and J. V. Sutcliffe, 1970, River flow forecasting through conceptual models. 1. A discussion of principles, J. Hydrology, 10(3), 282-290.

Pan, H.-L. and L. Mahrt, Interaction between soil hydrology and boundary-layer development, Bound.-Layer Meteorol., 38, 185-202.

Peck, E. L., 1976, Catchment modeling and initial parameter estimation for the National Weather Service River Forecast System, NOAA Tech. Memo., NWS HYDRO-31, Office of Hydrology, Washington, D.C.

Philip, J. R., 1969, Theory of Infiltration, in Advances in Hydroscience, vol 5 ed. by V. T. Chow, Academic Press, San Diego, pp. 215-296

Popov, E. G., 1963. Theory and practice problems in river runoff forecasting. Gidrometeoizdat, Moscow, USSR, (in Russian).

Russo, D. and E. Bresler, 1981a. Effect of field variability in soil hydraulic properties on solutions of unsaturated water and salt flows. Soil Sci. Soc. Am. J., 45, 675-681.

Russo, D. and Bresler, 1981b. Soil hydraulic properties as stochastic processes, 1, Analysis of field spatial variability. Soil Sci. Soc. Am. J., 45, 682-687.

SCS, 1972. National Engineering Handbook. Section 4, Hydrology. Soil Conservation Service USDA, US Government Printing Office, Washington, DC. USA.

Schaake, J. C. and C. Liu, 1989. Development and application of simple water balance models to understand the relationship between climate and water resources, Proceedings of the New Directions for Surface Water Modeling Symposium, Baltimore, May, 1989, IAHS Publ No 181, 343-352.

Schaake, J. C., 1990. From Climate to Flow, In Paul E. Waggoner (ed), Climate change and U.S. water resources, John Wiley & Sons, Inc., New York, 177-206.

Sellers, P. J., Y. Mintz, Y. C. Sud and A. Dalcher, 1986. A simple biosphere model (SiB) for use within general circulation models, J. Atmos. Sci., 43, 505-531.

Sherman, L.K., 1943, Comparison of F-curves derived by the method of Sharp and Holtan and of Sherman and Mayer, Eos Trans, AGU, 24, 465-467.

Sivapalan, M. and P. C. D. Milly, 1989, On the relation between the time condensation approximation and the flux-concentration relation,

J. Hydrol, 105, 357-367.

Smith, E. A., A. Y. Hsu, W. L. Crosson, R. T. Field, L. J. Fritschen, R. J. Gurney, E. T. Kanemasu, W. P. Kustas, D. Nie, W. J. Shuttleworth, J. B. Stewart, S. B. Verma, H. L. Weaver and M. L. Wesely, 1992. Area-average surface fluxes and their time-space variability over FIFE domain, J. Geophys. Res., 97(D17), 18,599-18,622.

Smith, R. E. and R. H. B. Hebbert, 1979. A Monte-Carlo analysis of the hydrologic effects on spatial variability of infiltration. Water Resour. Res., 15(2), 419-429.

Thomas, G. and A. Henderson-Sellers, 1987. Evaluation of satellite derived land cover characteristics for global climate modeling. Climate change, 11(3), 313-349.

Vieira, S. R., D. R. Nielsen and J. W. Biggar, 1981. Spatial variability of field measured infiltration rate. Soil Sci. Soc. Am. J., 45(6), 1040-1048.

Vinogradov, Y. B., 1988. Mathematical modeling of river runoff processes, Gidrometeoizdat, Leningrad, USSR, (in Russian).

WCRP, 1992. The Scientific Plan for the GEWEX Continental-Scale International Project (GCIP), WCRP-67 WMO/TD-No. 461, 65pp.

WCRP, 1993, Implementation Plan for GEWEX Continental-scale International Project: Volume 1: Data collection and operational model upgrade, IGPO Publication Series No. 6.

WMO, Intercomparison of conceptual models used in operational hydrological forecasting, Operational Hydrology Report No. 7, WMO-No. 429, Geneva.

Wood, E. F., M. Sivapalan, K. Beven and L. Band, 1988. Effects of spatial variability and scale with implications to hydrologic modeling. J. Hydrol., 102, 29-47.

Table 1. Descriptions of the three test basins

	French Broad Bird Creek	Leaf River	River
Location	Sperry, OK	Collins, MS	Rosman, NC
Latitude	36 16'42"	31 42'25"	35 17'56"
Longitude	-95 57'14"	-89 24'25"	-82 37'26"
Area (KM2)	2344	1924	176
Annual rainfall, P (MM)	963	1313	1916
Annual runoff, Q (MM)	220	428	1113
Annual evaporation, E (MM)	743	885	803
Annual potential evaporation, E_p (MM)	1312	1310	1113
Q/P	0.23	0.33	0.58
E/E_p	0.57	0.68	0.72
P/E_p	0.73	1.00	1.72
Data periods	10/01/55-09/30/62	10/01/52-09/30/69	10/01/53-09/30/64

Table 2. Summary of calibration and verification results

Error criterion	Model type	Bird Creek Calib period 55-60	Bird Creek Verif period 61-62	Leaf River Calib period 52-60	Leaf River Verif period 61-69	French Broad Calib period 54-59	French Broad Verif period 60-64
DRMS (CMS)	SWB	21.17	31.64	18.79	27.66	1.40	1.65
	SAC-SMA	18.61	31.45	16.04	21.05	1.31	1.34
	OSU	24.71	34.25	23.07	24.44	2.25	2.59
	Manabe	124.51	96.04	120.23	154.37	70.11	88.70
MVRMS (MM)	SWB	8.38	12.75	12.10	17.93	10.65	11.98
	SAC-SMA	6.07	11.13	10.12	14.09	9.54	9.86
	OSU	10.76	14.66	17.03	18.25	22.49	22.98
	Manabe	16.11	18.90	25.33	31.96	53.04	58.37
E	SWB	0.93	0.76	0.81	0.84	0.91	0.92
	SAC-SMA	0.94	0.75	0.88	0.88	0.92	0.94
	OSU	0.90	0.71	0.72	0.88	0.82	0.79
	Manabe	-1.57	-1.28	-6.68	-3.89	-12.81	-14.57

The OSU model was run at a time step of 1 hour by assuming the rainfall was evenly distributed over every 6 hours.

Table 3. Summary of hydrologic statistics for calibration and verification periods

Basin	Data Period	Rainfall	Potential EP	Discharge
Bird Creek	Calib 55-60	968	1395	220
	Verif 61-62	1079	1244	262
Leaf River	Calib 52-60	1279	1222	378
	Verif 61-69	1410	1223	558
French Broad	Calib 54-59	1834	1175	1054
	Verif 60-64	2006	1051	1186

Table 4. Bird Creek SWB parameters calibrated with different time steps

Time step (days)	$D_{b,max}$ (MM)	Q_{max} (MM/day)	$S_{max}/D_{b,max}$	$D_{u,max}/D_{b,max}$	$K_{dt'}$ (day^{-1})
0.25	262	4.52	0.598	0.014	3.08
0.50	247	4.36	0.590	0.016	3.53
1.00	265	4.02	0.538	0.012	3.63
2.00	245	4.80	0.650	0.037	3.55
4.00	276	20.0	0.769	0.084	2.61

Table 5. Bird Creek SWB performance statistics when calibrated with different time steps

Time step (days)	DRMS (CMS)	E (MM)	MVRMS (MM)
0.25	28.0	0.847	8.37
0.50	27.5	0.852	8.27
1.00	27.1	0.857	8.05
2.00	36.7	0.838	8.28
4.00	57.1	0.363	9.71

Table 6. Bird Creek SWB performance statistics when operated at different time steps using parameters calibrated at 1 day time step

Time step (days)	DRMS (CMS)	E (MM)	MVRMS (MM)
0.25	39.8	0.691	8.54
0.50	33.7	0.778	8.31
1.00	27.1	0.857	8.05
2.00	57.8	0.350	11.0
4.00	66.0	0.167	19.1

Table 7. Bird Creek SWB performance statistics when operated at different time steps using parameters calibrated at 6 hour time step

Time step (days)	DRMS (CMS)	E (MM)	MVRMS (MM)
0.25	28.0	0.847	8.37
0.50	29.4	0.831	8.32
1.00	37.9	0.720	8.17
2.00	61.7	0.260	11.0
4.00	65.2	0.188	18.9

Table 8. Bird Creek SWB performance statistics when operated at different time steps with uniform daily precipitation using parameters calibrated at 1 day time step

Time step (days)	DRMS (CMS)	E (MM)	MVRMS (MM)
0.25	47.1	0.568	13.0
0.50	39.8	0.690	9.81
1.00	27.1	0.857	8.05

Table 9. Bird Creek SWB performance statistics when operated at different time steps with uniform daily precipitation using parameters calibrated at 6 hour time step with actual 6 hour precipitation

Time step (days)	DRMS (CMS)	E (MM)	MVRMS (MM)
0.25	36.8	0.737	11.5
0.50	31.7	0.804	9.10
1.00	37.9	0.720	8.17

Table 10. Bird Creek SWB performance statistics when operated at different time steps with uniform daily precipitation using parameters calibrated at 6 hour time step with uniform daily precipitation

Time step (days)	DRMS (CMS)	E (MM)	MVRMS (MM)
0.25	27.6	0.852	7.76
0.50	33.3	0.789	12.0
1.00	49.4	0.527	10.8

Figure 1. Typical relationship of soil moisture deficit and evapotranspiration

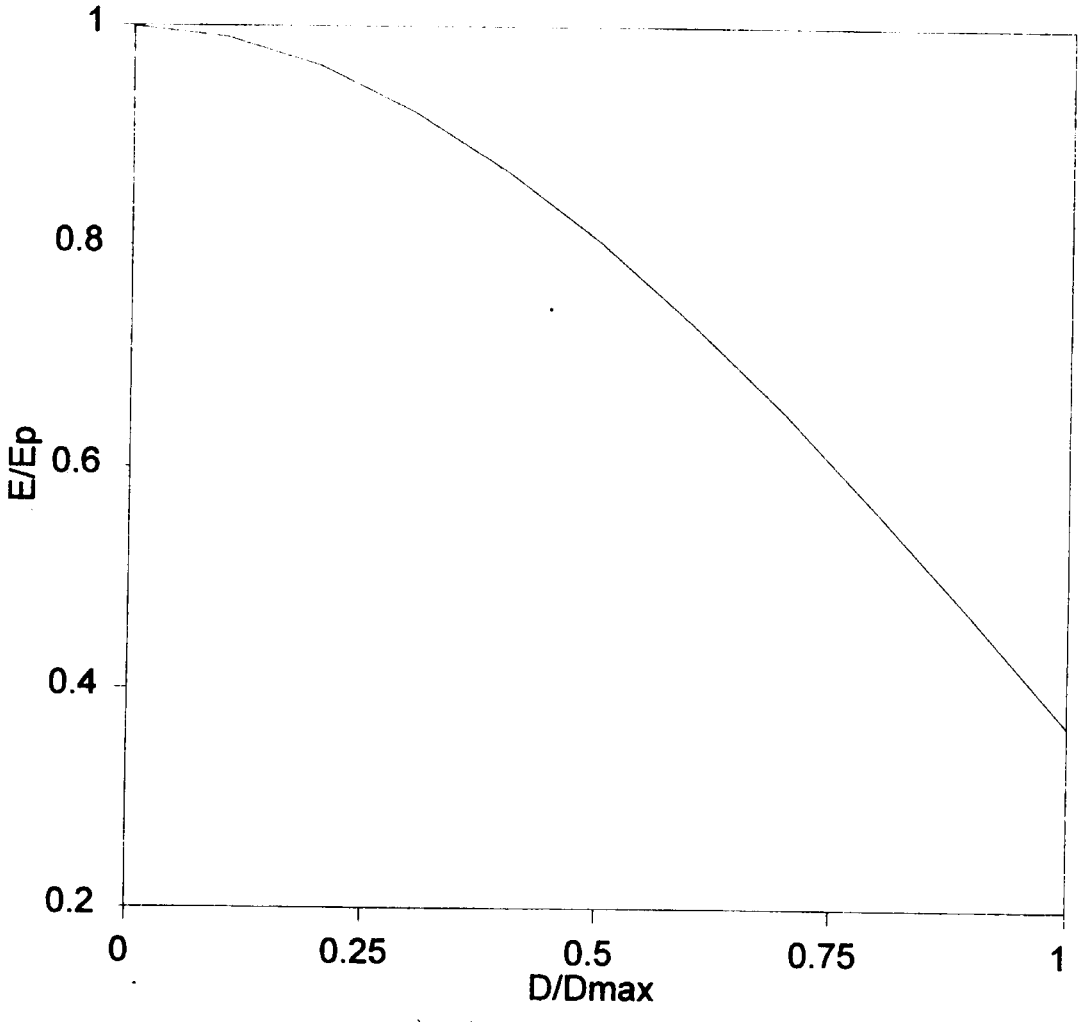

Figure 2. Distribution of hourly rainfall for the Medvenka River, USSR

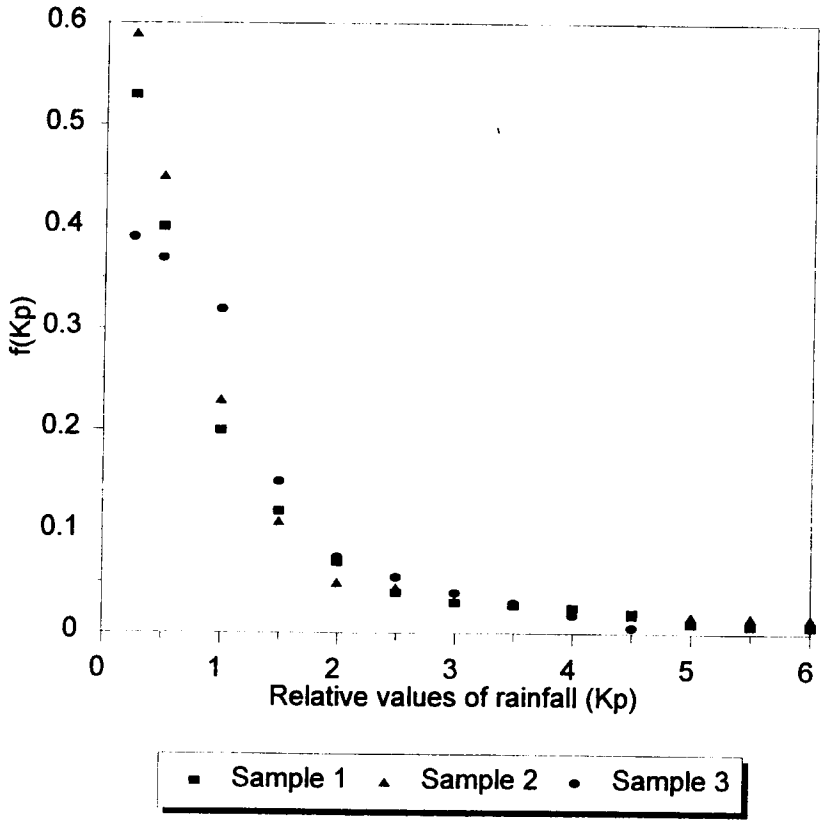

Figure 2. Distribution of hourly rainfall, the Medvenka River, Russia.

Figure 3. Comparison of simulated monthly runoff time series by SWB with observed monthly runoff

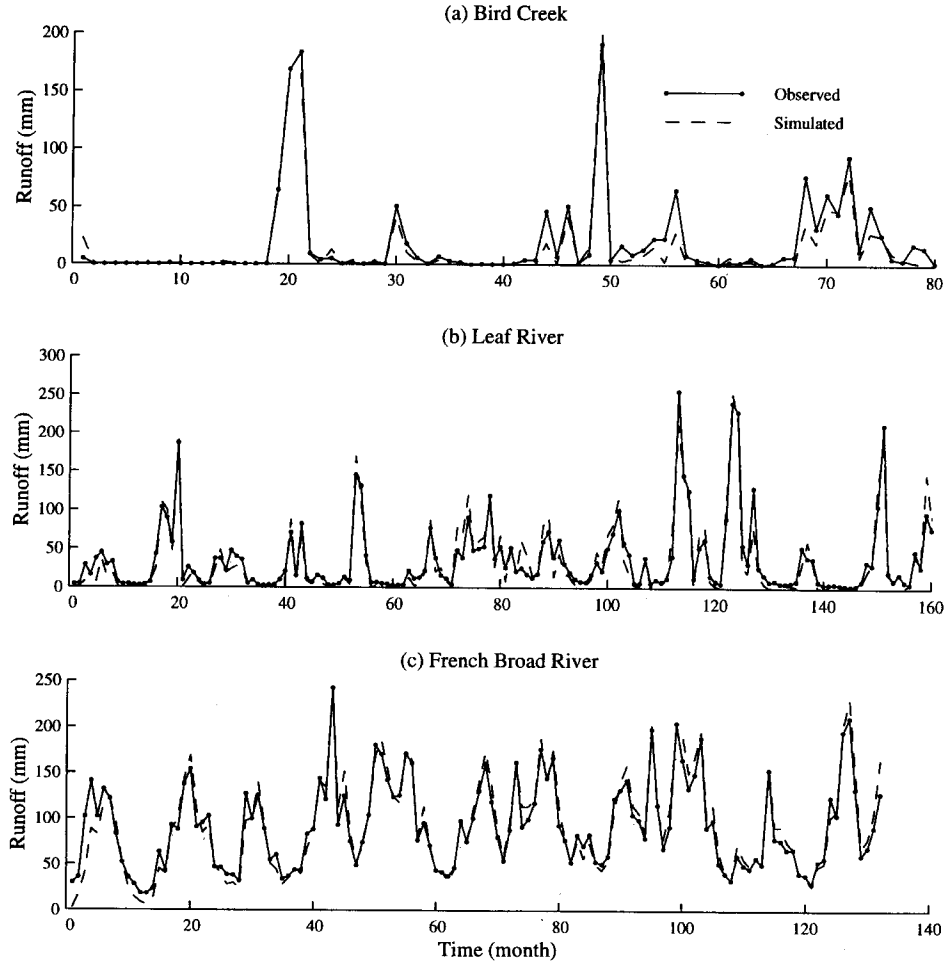

Figure 3. Comparison of simulated monthly runoff time series by simple water balance (SWB) with observed monthly runoff. (a) Bird Creek at Sperry, Oklahoma. (b) Leaf River near Collins, Mississippi. (c) French Broad River at Rosman, North Carolina.

Figure 4. Comparison of simulated daily streamflow discharge by SWB with observed daily discharge

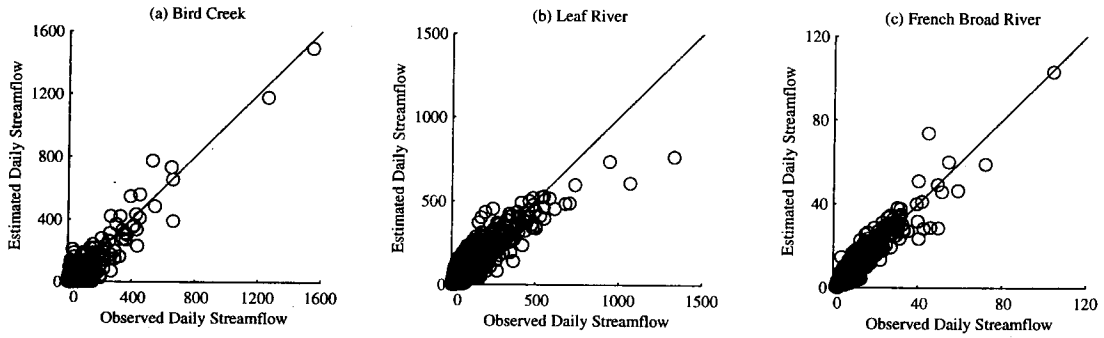

Figure 4. Comparison of simulated daily streamflow discharge by SWB with observed daily discharge. (a) Bird Creek at Sperry, Oklahoma. (b) Leaf River near Collins, Mississippi. (c) French Broad River at Rosman, North Carolina.

Figure 5. Comparison of simulated monthly runoff time series by SAC-SMA with observed monthly runoff

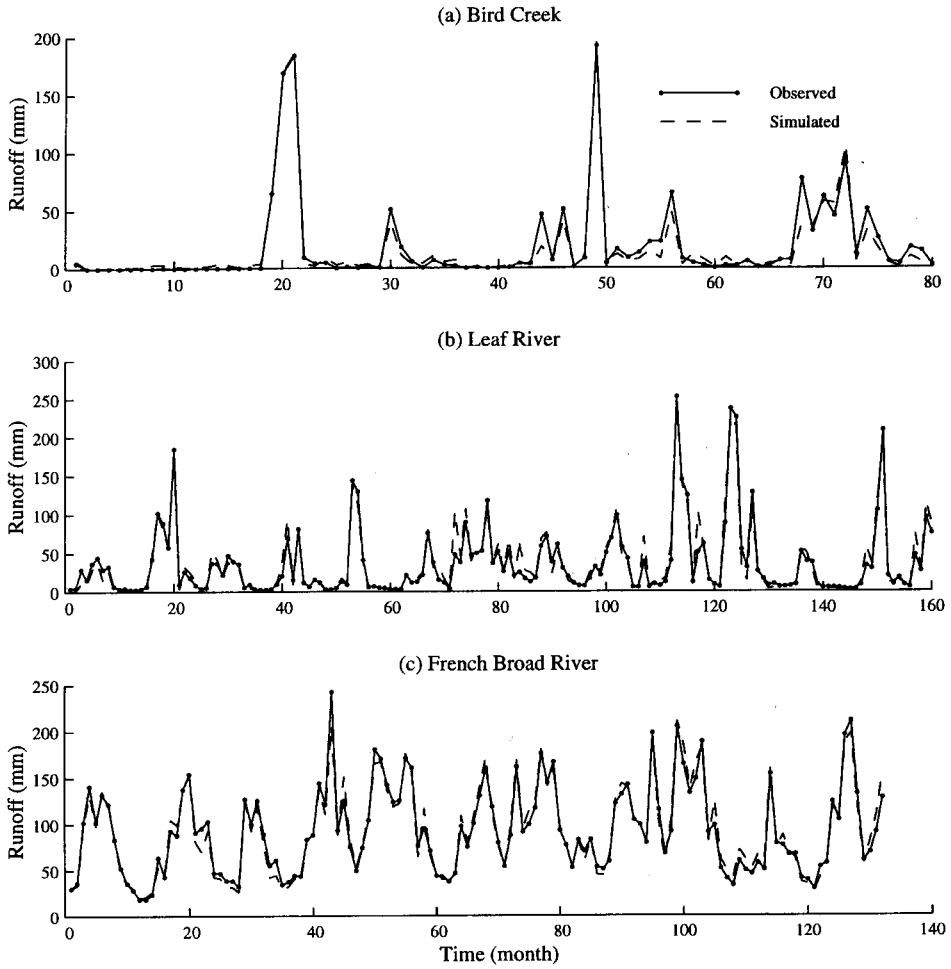

Figure 5. Comparison of simulated monthly runoff time series by SAC-SMA with observed monthly runoff. (a) Bird Creek at Sperry, Oklahoma. (b) Leaf River near Collins, Mississippi. (c) French Broad River at Rosman, North Carolina